

Journal of Visualized Experiments

Two peeling methods for the isolation of photoreceptor cell compartments in the mouse retina for protein analysis.

--Manuscript Draft--

Article Type:	Methods Article - JoVE Produced Video
Manuscript Number:	JoVE62977R1
Full Title:	Two peeling methods for the isolation of photoreceptor cell compartments in the mouse retina for protein analysis.
Corresponding Author:	Kasey Rose University of Southern California Los Angeles, CA UNITED STATES
Corresponding Author's Institution:	University of Southern California
Corresponding Author E-Mail:	kaseyvro@usc.edu
Order of Authors:	Kasey Rose Jeannie Chen Sowmya Lokappa
Additional Information:	
Question	Response
Please specify the section of the submitted manuscript.	Neuroscience
Please indicate whether this article will be Standard Access or Open Access.	Standard Access (\$1400)
Please confirm that you have read and agree to the terms and conditions of the author license agreement that applies below:	I agree to the Author License Agreement
Please provide any comments to the journal here.	
Please indicate the city, state/province, and country where this article will be filmed . Please do not use abbreviations.	LA, California
Please confirm that you have read and agree to the terms and conditions of the video release that applies below:	I agree to the Video Release

TITLE:

Two Peeling Methods for the Isolation of Photoreceptor Cell Compartments in the Mouse Retina for Protein Analysis

AUTHORS AND AFFILIATIONS:

Kasey Rose¹, Sowmya Lokappa¹, Jeannie Chen^{1,2*}

¹Zilkha Neurogenetic Institute, Keck School of Medicine, University of Southern California, Los Angeles, California, United States of America

²Department of Cell & Neurobiology, Keck School of Medicine, University of Southern California, Los Angeles, California, United States of America

Corresponding Author:

Jeannie Chen (jeannie@usc.edu)

Email Addresses of Co-Authors:

Kasey Rose (kaseyvro@usc.edu)

Sowmya Lokappa (slokappa@usc.edu)

Jeannie Chen (jeannie@usc.edu)

SUMMARY:

This protocol presents two techniques to isolate the subcellular compartments of murine rod photoreceptors for protein analysis. The first method utilizes live retinæ and cellulose filter paper to separate rod outer segments, while the second employs lyophilized retinæ and adhesive tape to peel away rod inner and outer segment layers.

ABSTRACT:

Rod photoreceptors are highly polarized sensory neurons with distinct compartments. Mouse rods are long (~80 µm) and thin (~2 µm) and are laterally packed in the outermost layer of the retina, the photoreceptor layer, resulting in alignment of analogous subcellular compartments. Traditionally, tangential sectioning of the frozen flat-mounted retina has been used to study the movement and localization of proteins within different rod compartments. However, the high curvature of the rod-dominant mouse retina makes tangential sectioning challenging. Motivated by the study of protein transport between compartments, we developed two peeling methods that reliably isolate the rod outer segment (ROS) and other subcellular compartments for western blots. Our relatively quick and simple techniques deliver enriched and subcellular-specific fractions to quantitatively measure the distribution and redistribution of important photoreceptor proteins in normal rods. Moreover, these isolation techniques can also be easily adapted to isolate and quantitatively investigate the protein composition of other cellular layers within both healthy and degenerating retinæ.

INTRODUCTION:

Rod photoreceptor cells, tightly packed in the outermost layer of the neural retina, are an integral part of dim light vision. To function as faithful photon counters, rods utilize a G-protein-based

signaling pathway, termed phototransduction, to generate rapid, amplified, and reproducible responses to single photon capture. This response to light ultimately triggers a change in the current at the plasma membrane and is subsequently signaled to the rest of the visual system¹. As their name implies, each rod cell has a distinct rod-like shape and exhibits a highly polarized cellular morphology, consisting of an outer segment (OS), inner segment (IS), cell body (CB), and synaptic terminal (ST). Each subcellular compartment has specific protein machinery (membrane-bound and soluble), biomolecular features, and protein complexes that play crucial roles such as visual phototransduction, general housekeeping and protein synthesis, and synaptic transmission^{2,3}.

Over 30 years ago, the light-dependent reciprocal movement of subcellular proteins, specifically transducin (away from the OS) and arrestin (towards the OS), was first observed⁴⁻⁷. Early on, this observed phenomenon was received with skepticism, due in part to immunohistochemistry's vulnerability to epitope masking⁸. In the early 2000s, stimulus-dependent protein translocation was confirmed by using a rigorous and arduous physical sectioning technique⁹. Serial tangential sectioning of the frozen flat-mounted rodent retinæ followed by immunoblotting revealed that transducin^{9,10}, arrestin^{11,12}, and recoverin¹³ all undergo subcellular redistribution in response to light. It is believed that light-driven translocation of these key signaling proteins not only regulates the sensitivity of the phototransduction cascade^{9,14,15}, but may also be neuroprotective against light damage¹⁶⁻¹⁸. Because light-driven protein transport in rods appears to be very significant to rod cell biology and physiology, techniques that permit the isolation of different subcellular compartments to determine protein distribution are valuable research tools.

Currently, there are a few methods aimed at isolating the rod subcellular compartments. However, these methods can be lengthy and difficult to reproduce, or require a sizable amount of retinal isolate. Rod outer segment (ROS) preparations *via* density gradient centrifugation¹⁹, for example, is commonly used to separate the ROS from retinal homogenate. This method is widely used for western blot, but the procedure is very time consuming and requires a minimum of 8–12 murine retinæ²⁰. On the other hand, serial tangential sectioning of frozen murine and rat retinæ has been successfully implemented in isolating the OS, IS, CB, and ST^{9,11,13}. However, this method is technically challenging due to the necessity of fully flattening the small and highly curved murine retina to align the retinal layers prior to tangential sectioning. Since there are a plethora of mouse models and transgenic mice recapitulating diseases of the visual system, the creation of a technique that reliably, quickly, and easily separates individual rod compartments holds promise in revealing the physiologic processes that occur in each specialized compartment and the mechanisms that underlie visual processes in health and disease.

To facilitate these investigations, we describe two peeling methods that isolate rod subcellular compartments more easily than current protocols. The first peeling method, adapted from a technique to expose fluorescently labeled bipolar cells for patch clamp recording²¹, employs cellulose filter paper to sequentially remove the ROS from a live, isolated murine retina (**Figure 1**). The second method, adapted from a procedure that isolates the three primary retinal cell layers from a chick²² and frog²³ retina, utilizes adhesive tape to remove the ROS and rod inner segment (RIS) from a lyophilized retina (**Figure 2**). Both procedures can be completed in 1 h and

are considerably user-friendly. We provide validation of the effectiveness of these two separation protocols for western blot by utilizing dark-adapted and light exposed retinae from C57BL/6J mice to demonstrate light-induced translocation of rod transducin (GNAT1) and arrestin (ARR1). Moreover, using the tape peeling method, we provide additional evidence that our technique can be used to examine and address inconsistencies between protein localization data acquired by immunocytochemistry (ICC) and western blots. Specifically, our technique showed that: 1) the protein kinase C- α (PKC α) isoform is present not only in bipolar cells, but also in murine ROS and RIS, albeit in low concentrations^{24,25}, and 2) rhodopsin kinase (GRK1) is present predominantly in the isolated OS sample. These data demonstrate the effectiveness of our two peeling techniques for separating and quantifying specific rod and retinal proteins.

PROTOCOL:

All experiments were performed according to the local institutional guidelines of the committee on research animal care from the University of Southern California (USC).

1. Live cell retinal peeling method

1.1. Preparation of Ames' Buffers, Peeling Papers, and Dissection Dish

1.1.1. Using blunt tip iris scissors (or equivalent scissor type), cut the cellulose filter paper (Grade 413) into rectangles measuring approximately 5 mm x 2.5 mm. Store the cuttings for future use.

1.1.2. Prepare 1 L of Ames' HEPES buffer by combining one bottle of Ames' Medium, 2.38 g HEPES, and 0.877 g of NaCl. Dissolve the reagents in a sterile glass bottle with distilled ultrapure water and adjust the osmolarity and pH to 280 mOsm and 7.4, respectively. Filter to sterilize (pore size 0.2 μ m), seal the lid with paraffin film, and store at 4 °C.

1.1.3. Prepare 1 L of Ames' bicarbonate buffer by combining one bottle of Ames' Medium and 1.9 g of NaHCO₃. Dissolve the reagents in a sterile glass bottle with distilled ultrapure water and adjust the osmolarity and pH to 280 mOsm and 7.4, respectively. Filter to sterilize (pore size 0.2 μ m), seal the lid with paraffin film, and store at 4 °C.

NOTE: Ames' HEPES and Ames' bicarbonate buffers can be prepared in advance and stored for 1 week at 4 °C.

1.1.4. At the bottom of a 35 x 10 mm Petri dish, create a lattice or checkerboard pattern with a scalpel (blade No. 11, 40 mm).

NOTE: The textured bottom of the Petri dish holds the isolated, free-floating eye in place during the retinal dissection.

1.2. Dissection of the retina

NOTE: For this procedure, the buffer should be brought to and kept at room temperature (RT). Refresh the Ames' bicarbonate buffer every 15 min with fresh carbogenated Ames' bicarbonate buffer during the dissection. This maintains the necessary physiologic pH.

1.2.1. Around 15–20 min before the dissection, oxygenate the Ames' HEPES buffer in a 100 mL laboratory or media bottle equipped with a tubing cap adapter and bubble the Ames' Bicarbonate buffer with 95% O₂ and 5% CO₂ in a tissue incubation chamber and in a 100 mL laboratory or media bottle equipped with a tubing cap adapter.

1.2.2. Euthanize an equal number of both genders of C57BL/6J mice (2-3 months old) either by isoflurane inhalation or carbon dioxide (CO₂) followed by cervical dislocation. Eucleate the eyes with curved scissors and place the eyes into the textured 35 x 10 mm Petri dish filled with bubbled Ames' bicarbonate buffer.

1.2.3. Create an eye cup (**Figure 1A**) by puncturing a hole at the cornea-limbus junction with an 18 G needle. Cut along the perimeter of this junction using micro-dissection iris scissors to remove the cornea of each eye. Separate the lens and vitreous humor from each eye using tweezers and discard.

1.2.4. Isolate the retina from the eye cup by carefully peeling the retinal pigmented epithelium (RPE)-sclera-choroid complex away from the neural retina. Discard the RPE-sclera-choroid complex. Ensure that the retina is not damaged during the dissection by handling only the edges.

1.2.5. Transfer isolated retinæ using a wide bore transfer pipette into the lid of a 60 x 15 mm dish filled with bubbled Ames' bicarbonate buffer.

1.2.6. Orient the hemisphere-shaped retina concave up (the photoreceptors are pointing upward) and bisect each retina (through the optic nerve) using iris scissors or a scalpel (blade No. 10, 40 mm). Trim the curved edges of each half retina to make two rectangles (**Figure 1A**).

NOTE: Minimizing the curvature of each halved retina allows for the retina to flatten better in subsequent peeling steps and produces an accurate peel of the rod outer segment (ROS) layer.

1.2.7. Store the halved retinæ in the tissue incubation chamber that is continuously bubbled with 95% O₂ and 5% CO₂.

NOTE: Isolated retinæ can be kept in the carbogenated Ames' bicarbonate buffer for ~24 h.

1.3. Rod outer segment (ROS) collection by filter paper peeling

NOTE: Refresh the RT oxygenated Ames' HEPES buffer every 15–20 min during the peeling process to maintain the necessary physiologic pH.

1.3.1. Transfer one retinal rectangle from the tissue chamber with a wide bore transfer pipette and a 5 mm x 2.5 mm piece of filter paper into a 35 x 10 mm Petri dish filled with Ames' HEPES

buffer bubbled with 100% O₂.

1.3.2. Orient the partitioned retina concave up and ensure the photoreceptors are facing down toward the bottom of the dish. Lightly grasp the sides of the halved retina with tweezers and move it on top of the filter paper. Once the retina is centered on the filter paper, move the filter paper upward so the halved retina touches the filter paper to create the ROS-to-filter paper adhesion (**Figure 1B**).

NOTE: Make sure that the photoreceptor layer makes direct contact with the filter paper.

1.3.3. Carefully lift the filter paper with the attached retina out of the Ames' HEPES buffer. Place the bottom side of the filter paper (the side without the retina) on a paper towel and dab 2–3 times to dry (**Figure 1B**).

1.3.4. Add a drop of Ames' HEPES onto the side of the filter paper with the retina. Place the filter paper on the paper towel again to dry, as just described. Repeat this process two more times.

1.3.5. Place the filter paper with the retina back into the Petri dish. Using tweezers, gently push all edges of the halved retina up and away from the filter paper on all sides.

1.3.6. Delicately peel the retina away from the filter paper. Touch only the extreme perimeter of the retina during the peeling process to preserve the retina's structural integrity.

1.3.7. Lift the filter paper from the Petri dish and remove excess liquid on a paper towel. Make sure the side that was in contact with the retina does not contact the paper towel.

1.3.8. Place the filter paper with the partial ROS layer into a labeled tube on ice (**Figure 1B**). Keep the peeled retina submerged in Ames' HEPES buffer.

1.3.9. Repeat the peeling process for this halved retina approximately 7–8 times to remove the entire ROS layer. After each peel, place the filter paper into the same tube, which will contain the isolated ROS from one halved retina.

NOTE: Take care to not tear the halved retina when peeling it away from the filter paper, as the retina becomes thinner during this process.

1.3.10. Place the tube containing all filter paper peels of the isolated ROS on ice for immediate use or freeze directly on dry ice and store at -80 °C.

1.3.11. Use tweezers to transfer the leftover peeled retina (lacking ROS) into an appropriately labeled tube. Place the tube on ice for immediate use or freeze with dry ice and store at -80 °C.

1.3.12. Repeat the peeling process for each halved retina and accurately label each tube.

2. Lyophilized retina peeling method

2.1. Buffers, peeling medium, dissection dish preparation, and lyophilizer set-up

2.1.1. In a 1 L storage bottle, prepare the Ringer's solution by adding 500 mL of distilled ultrapure water. Dissolve the reagents to reach a final concentration of 130 mM NaCl, 3.6 mM KCl, 2.4 mM MgCl₂, 1.2 mM CaCl₂, 10 mM HEPES, and 0.02 mM EDTA. Adjust the pH to 7.4 with NaOH, add ultrapure water to bring the final volume to 1 L, and adjust osmolarity to 313 mOsm.

2.1.2. Prior to the use, filter the Ringer's solution with a sterile filter (pore size 0.2 µm), seal the lid with paraffin film, and store at 4 °C.

2.1.3. Using blunt tip iris scissors (or equivalent scissor type), cut the cellulose filter paper into rectangles measuring approximately 5 mm x 2.5 mm. Use a pencil to write on one side of the filter paper to create a unique label.

2.1.4. Create a lattice or checkerboard pattern in the bottom of a 35 x 10 mm Petri dish using a scalpel (blade No. 11, 40 mm).

2.1.5. Turn on the lyophilizer according to the manufacturer's specifications.

2.1.6. Acquire liquid nitrogen in a Dewar flask or similar insulating vacuum flask.

2.2. Retinal dissection

2.2.1. Complete the retinal dissection as described in section 1 of the protocol (**Figure 1A**). Use cold Ringer's solution instead of Ames' buffer.

2.2.2. Post dissection, store the halved, rectangular retinae in a 35 x 10 mm Petri dish filled with cold Ringer's solution and place on ice.

2.3. Retinal sample preparation for lyophilization

2.3.1. Place a 5 x 2.5 mm piece of filter paper and transfer a halved retina into the texturized 35 x 10 mm Petri dish filled with cold Ringer's buffer. Use a wide bore transfer pipette to move each retina between dishes.

2.3.2. Use tweezers to carefully flip the retina so it is oriented concave up (the photoreceptors are pointing upward) and move it so it rests on top of the filter paper (**Figure 2A**).

NOTE: Make sure the photoreceptors do not contact the filter paper (the retinal ganglion cell layer should be in direct contact with the filter paper) and the unique label is visible. To easily and quickly identify the retinal isolate, it is recommended that the unique label should be located on the underside of the filter paper.

2.3.3. Lift the filter paper by the edges upward so the halved piece of retina touches the filter paper and continue to lift the filter paper out of the Ringer's solution.

2.3.4. Place the bottom side of the filter paper (the side without the retina on it) on a paper towel and carefully dab 2–3 times to remove excess liquid (**Figure 2A**).

2.3.5. Pick up the filter paper with tweezers and add a drop of cold Ringer's onto the side of the filter paper with the retina. Place the filter paper on the paper towel again to remove excess liquid. Repeat the process two more times.

NOTE: These alternating wetting and drying steps ensure that the tissue is firmly attached to the filter paper.

2.3.6. Store each adhered retina/filter paper sample in a Petri dish filled with cold Ringer's until ready to freeze all samples. Repeat this process for all halved retinas.

2.3.7. Obtain a clean and dry 35 x 10 mm Petri dish (bottom only) and a piece of aluminum foil cut into a 3.5 x 3.5 inch square.

2.3.8. Lift each sample out of the cold Ringer's buffer with tweezers. Ensure that the tweezers contact only the filter paper edges, avoiding the halved retina.

2.3.9. Place the bottom side of each filter paper (the side without the retina on it) on a paper towel and remove excess liquid.

2.3.10. Add a drop of cold 1x PBS (137 mM NaCl, 2.7 mM KCl, 10 mM Na₂HPO₄, 2 mM KH₂PO₄, pH 7.4) onto the side of the filter paper where the retina is adhered. Dab the filter paper on the paper towel to remove excess liquid.

NOTE: Make sure that the moisture from the filter paper is sufficiently removed before freezing.

2.3.11. Place all filter paper pieces into the 35 x 10 mm Petri dish. Use a lint free tissue paper to wick away any excess liquid surrounding the filter paper.

NOTE: Do not overcrowd the Petri dish with samples. If more than four murine eyes are used, consider using a larger Petri dish or multiple smaller Petri dishes to hold the retina/filter paper samples.

2.3.12. Tightly wrap the entire dish with aluminum foil. Ensure that the edges of the aluminum foil are secured and smoothly pressed into the bottom of the Petri dish. Puncture a handful of 0.1–0.2 mm holes into the aluminum foil lid (**Figure 2A**).

2.3.13 Using metal tongs, gradually lower the aluminum foil covered Petri dish into the liquid nitrogen. Keep the samples in the liquid nitrogen (<10 min) until ready to lyophilize.

2.4. Lyophilization

2.4.1. Place the aluminum foil covered Petri dish into a freeze-drying flask and attach it to the lyophilizer machine following the manufacturer's protocol. Lyophilize the retinae for 30 min.

2.4.2. Detach the flask from the lyophilizer and shut off the machine according to the manufacturer.

2.4.3. Remove the aluminum foil and either work with the freeze-dried samples the same day or store them in properly labeled 1 mL microcentrifuge tubes. Place these tubes in a container (such as a 50 mL conical tube) filled with an anhydrous desiccant and store the samples at -80 °C.

2.5. Rod outer and inner segment collection by adhesive tape peeling.

2.5.1. Cut strips of clear adhesive tape (1–2 cm) and store strips on the edge of the tape dispenser/lab bench/etc. for quick use.

2.5.2. Move one retinal sample to the lid of a plastic 60 x 15 mm Petri dish for peeling. Ensure to only grab the outermost edges of the filter paper and avoid touching the retina.

2.5.3. Using blunt tip iris scissors (or equivalent scissor type), cut a small rectangular piece of tape to the approximate size of the tissue (1.5 x 2.5 mm).

2.5.4. Carefully lay a small piece of tape on top of the lyophilized retina (**Figure 2B**) and apply slight pressure with the tweezers to make sure it bonds with the photoreceptor layer (the orange/pink-tinted top layer).

2.5.5. Slowly peel the tape away. Both the rod outer segment (ROS) and rod inner segment (RIS) will be adhered to the tape (**Figure 2B**).

2.5.6. Ensure that there is a thin white film at the fractured surface. This is RIS. To separate the RIS, place another piece of tape and push the tape down on the fractured surface (**Figure 2B**).

NOTE: It may take more than one piece of tape to remove the entire thin white layer.

2.5.7. Place the piece of tape with only the orange/pink layer into a microcentrifuge tube labeled +ROS.

2.5.8. Place the tape or pieces of tape with the thin white layer into a microcentrifuge tube labeled +RIS.

NOTE: Separating the lyophilized retina with tape takes practice. The amount of pressure applied to the tape will affect how the lyophilized sample will fraction. If too much pressure is placed on the tape over the sample, the whole lyophilized retina will peel off the filter paper and will stick to the tape. If too little pressure is added to the tape, the orange/pink top layer (+ROS) will not stick to the tape.

2.5.9. Collect the leftover retinal tissue (bereft of ROS and RIS layers, -OIS) located on the filter paper by peeling off the thick, white layer from the filter paper using tape. Place the isolate into a tube labeled -OIS.

2.5.10. Repeat these steps for each halved retinal sample.

2.5.11. Store the isolated layers from the lyophilized retinae either at room temperature if performing protein quantification, gel electrophoresis, and protein immunoblots that same day, or store in a container (such as 50 mL conical tube) filled with anhydrous desiccant at -80 °C for later use.

3. Western blot sample preparation for peeling isolations

3.1. Prepare RIPA lysis buffer

3.1.1. In a 100 mL storage bottle, add reagents to obtain a final concentration of 50 mM Tris-HCl pH 7.4, 150 mM NaCl, 1% Triton X-100, 1% Sodium deoxycholate, 0.1% SDS, and 1 mM EDTA. Add 100 mL of deionized ultrapure water and mix thoroughly.

NOTE: RIPA lysis buffer can be stored at 2–8 °C for 2–3 weeks. For longer storage, aliquot and store in the -20 °C freezer.

3.1.2. On the day of the experiment, add a protease inhibitor cocktail (0.1 M PMSF, 1:1000 Aprotinin, and 1:1000 Leupeptin) to the RIPA lysis buffer and keep on ice.

3.2. Filter paper peeling lysate preparation for western blot

3.2.1. Ensure that tubes containing the filter paper peels and leftover peeled retinae are maintained on ice (for the experiment on the same day) or removed from -80 °C freezer storage and placed on ice.

3.2.2. Remove any excess liquid from the bottom of the microcentrifuge tubes containing the filter paper peels. Quickly spin in a mini centrifuge for 2–4 s and discard any remaining liquid.

3.2.3. Pipette 45–55 µL of cold RIPA buffer into tubes containing the filter paper isolate.

3.2.4. Homogenize each sample with a clean, autoclaved pestle mixer for 1 min. Make sure the filter paper stays in contact with the pestle mixer. Keep the filter paper on the side of each tube rather than at the bottom.

3.2.5. With tweezers, move the filter papers to the side of each tube and spin in the mini centrifuge for 2–4 s. This will remove the RIPA buffer from the filter paper.

3.2.6. Remove dried filter paper and repeat for all filter papers within each tube if necessary.

3.2.7. Transfer the homogenate to a new tube and label it appropriately.

NOTE: This is the most time-consuming step, and if not completed properly, much of the sample will end up being absorbed by the filter paper.

3.2.8. Pipette 60–80 μ L of cold RIPA buffer into the individual tubes with the leftover peeled retinae.

3.2.9. Homogenize each sample with a clean, autoclaved pestle mixer for 1 min.

3.3. Tape peeling Lysate preparation for western blot

3.3.1. Place the RT lyophilized samples or the -80 °C samples on ice.

3.3.2. Pipette 50–70 μ L of cold RIPA buffer into each tube containing +ROS and +RIS tape peels.

3.3.3. Pipette 60–80 μ L of cold lysis buffer into the -OIS tubes containing the remaining lyophilized retina, with the ROS and RIS removed.

3.3.4. Homogenize each sample with a clean pestle mixer for 1 min. Ensure that the tape in the individual tubes stays in contact with the pestle mixer and lysis buffer.

3.3.5. With sterilized tweezers, move the tape to the side of the tubes and spin with a mini centrifuge for 2–4 s. This will remove the liquid from the tape. Remove the dried tape from the tubes.

NOTE: At this point, you may combine two half retinal isolates from the same retina for either the ‘filter paper peeling’ or ‘tape peeling’ method to ensure you have enough volume to perform a bicinchoninic acid assay (BCA).

REPRESENTATIVE RESULTS:

The present strategies were developed to provide relatively rapid and simple methods to isolate and analyze proteins among specific rod subcellular compartments for western blot analysis. We applied two sequential peeling techniques (**Figure 1** and **Figure 2**) followed by immunoblotting to demonstrate that these methods could reliably be used to detect the known distribution of

rod transducin (GNAT1) and arrestin (ARR1) in both dark- and light-adapted animals. To validate the effectiveness of our two protocols in precisely isolating rod subcellular compartments without contamination from other cellular layers, immunoblots were probed with antibodies for cytochrome C (Cyt C), actin, and Gβ5S/Gβ5L²⁶. A list of antibodies and dilutions used is presented in **Table 1**. Cyt C and actin indicated ROS purity, as they are abundant proteins in the proximal retina but are absent in the ROS. Gβ5L, a component of GTPase activating protein (GAP) for GNAT1²⁷, is present in the ROS and RIS and served as a control for these isolations. Gβ5S, the shorter splice isoform that is not present in ROS or RIS but is in all other rod compartments, served as a control for non-ROS/RIS isolated subcellular compartments.

First, the effectiveness of our sequential live cell retinal peeling method was assessed by analyzing the distribution of GNAT1 and ARR1 in rods of dark- and light-adapted mice (**Figure 3**). The filter papers containing the ROS (+ROS) were pooled from a total of one whole retina, and the corresponding residual tissue (-ROS) was also combined. The signals from the indicated proteins were subsequently compared between the +ROS samples and the -ROS samples, and a whole isolated retina served as input control. Protein concentration and homogenization volume for these samples are presented in **Table 2**. Results presented in **Figure 3A** show that, in dark-adapted animals, the distribution of GNAT1 and ARR1²⁸ closely matched their known dark-state distributions where the GNAT1 signal was visibly the strongest in the +ROS isolation, whereas the ARR1 signal was more robust in the -ROS isolation. Accordingly, in the light-exposed retinæ, the GNAT1 signal was noticeably reduced in the +ROS isolation and had an increased signal in the -ROS sample, while light-induced ARR1 translocation could be visualized in +ROS and -ROS samples. Results from six different experiments were quantified, and statistically significant differences were found between dark/light conditions for GNAT1 and ARR1 in the +ROS and -ROS samples (**Figure 3B**). These findings are consistent with the previously known protein light/dark movement within rod subcellular compartments and strongly indicate that this technique can isolate enriched +ROS fractions.

To further validate our live cell peeling method, we investigated known ROS purity marker distributions in both +ROS and -ROS samples. In both dark- and light-adapted samples, the Gβ5S, Cyt C, and actin signals are excluded from the +ROS samples (**Figure 3A**), demonstrating an absence of contamination from other cellular layers. Additionally, the Gβ5L signal was clearly visible in the +ROS samples (**Figure 3A**). Furthermore, actin and Gβ5L signals not only confirmed the purity of the +ROS and -ROS fractions, but also acted as controls for normalization, with the signals from the +ROS samples being normalized against Gβ5L and -ROS samples being normalized against actin. As presented in **Figure 3A**, it is recommended that the live cell peeling isolates are loaded alongside a loading control, specifically a whole retinal homogenate, for optimal immunoblotting normalization and analysis. Together, these data validate that our live cell peeling method can provide a rapid and reproducible approach to isolate the ROS subcellular layer from the rest of the rod and retina for protein analysis.

We next evaluated our lyophilized peeling technique to verify that this method could reproducibly isolate the ROS and RIS compartments. Prior to immunoblotting, we imaged the surfaces of intact and peeled lyophilized mouse retinæ using a scanning electron microscope

(SEM) to analyze which photoreceptor subcellular layer the tape peeling yielded (**Figure 4**). Before peeling with adhesive tape, the surface of the intact lyophilized retina (orange/pink-tinted layer) closely matched the profile of the characteristic cylindrical ROS (**Figure 4A**). After the initial tape peel, the ROS and RIS appeared to be fully removed, as evidenced by the uniform nuclear layer present on the surface of the leftover peeled lyophilized retina (**Figure 4C**). Subsequent tape peels removed the RIS (thin white layer, **Figure 4B**) from the free surface of the peeled layer, a process likely aided by the narrow and fragile connecting cilium linking the inner and outer segments. These results confirmed that rod subcellular layers from lyophilized retinal tissue can be specifically fractionated using tape.

Having validated the effectiveness of this method visually, dark- and light-adapted peeled retinae were subjected to immunoblotting using the same approach utilizing protein markers for different compartments as outlined for our live cell peeling method (**Figure 3**). Protein concentration and homogenization volume for ROS isolation (+ROS), RIS isolation (+RIS), and the remaining retinal layers (-OIS) are presented in **Table 2**. As expected, there was a clear light-induced shift for GNAT1 from the ROS to the RIS, as well as ARR1 from the RIS to the ROS (**Figure 5A**). GNAT1 was most abundant in the +ROS sample in the dark and the +RIS sample in the light, while ARR1 signal was reversed (**Figure 5A**). We next normalized and quantified the translocating protein signals from +ROS, +RIS, and -OIS isolations (**Figure 5B**), using the same controls and approach as the live peeling methodology. We also combined +RIS and -OIS samples (**Figure 5C**) for a more direct comparison to our live cell filter paper peeling method (**Figure 3B**). Both graphs show the well-established and characteristic light-induced translocation of both GNAT1 and ARR1. Based on these observations, the tape peeling preparation appears to yield enriched ROS and RIS fractions, as evidenced by the protein composition of ARR1 and GNAT1 in these isolations.

Next, the purity of individual subcellular isolations was evaluated. Similar to the results shown in **Figure 3A**, the +ROS samples lacked signals for actin, cytochrome C, and G β 5S while displaying a strong G β 5L signal (**Figure 5**). This finding shows a lack of contamination from other subcellular compartments in our +ROS sample preparation. The protein content of the subsequent subcellular layer of the rod, the +RIS isolation, was then assessed. We found that the +RIS sample was positive for Cyt C, G β 5L, and actin. This finding is consistent with the known composition of RIS, which is rich in mitochondria and cytoskeletal elements. The final layer, the -OIS isolate, had protein distributions consistent with the -ROS samples shown in **Figure 3A**.

To further assess the utility of our adhesive tape peeling method in investigating rod subcellular compartments' protein compositions, we specifically examined the immunoreactivity of rhodopsin kinase (GRK1) and protein kinase C- α (PKC α) in our +ROS, +RIS, and -OIS samples. Different experimental methods, such as immunocytochemistry (ICC) and western blot, often yield conflicting results about the precise localization of these proteins in rods and the retina. GRK1, for example, is thought to be relatively abundant in rod and cone OS to mediate phosphorylation of light-activated opsins²⁹. However, immunolabeling of retinal slices has revealed the localization of GRK1 either specifically in the OS^{30,31} or throughout the entire photoreceptor layer³². PKC α , on the other hand, is a protein that is commonly used for ICC to

label bipolar cells. Despite no clear evidence of rod-specific PKC α immunolabeling in retinal slices²⁵, there is considerable biochemical^{24,25} and functional³³⁻³⁵ evidence that supports the presence and phosphorylating role of PKC α in the ROS. Utilizing our technique, we found that GRK1 immunoreactivity was most intense in the +ROS samples in light-exposed retinæ and was absent in -OIS samples (**Figure 6A**). Conversely, we show that the +ROS and +RIS samples displayed a faint signal for PKC α . As can be seen in **Figure 6B**, PKC α is commonly not detected in the ROS or RIS by immunofluorescence staining of retinal sections. However, PKC α was immunodetected by western blot (**Figure 6A,D**). Because the +ROS and +RIS isolations display a strong G β 5L signal and an absence of G β 5S (**Figure 6A**), we are confident that the dim PKC α signal in both ROS and RIS samples is genuine and not due to contamination from other layers. To visualize the individual signals in +ROS, +RIS, and -OIS isolations, GRK1 and PKC α blots were combined and plotted for comparison (**Figure 6C**).

Lastly, an example of a sub-optimal peeling session (**Figure 6D**) demonstrates how contamination from different sub-layers can skew results, further illustrating the importance of data interpretation and inclusion of the appropriate control antibodies to screen for experimental peeling errors. In this tape peeling isolation example, a faint G β 5S signal is evident in the RIS isolation lane, indicating slight contamination from the -OIS sample. Depending on the user's goal, this slight contamination may not be an issue. However, in this case, we were investigating the PKC α signal in +ROS and +RIS samples, and the PKC α signal is slightly higher in the RIS lane compared to the ROS lane (**Figure 6A,D**), perhaps due to contamination. Thus, care should be taken during the peeling process to ensure an accurate isolation and to minimize contamination. Despite minimal contamination due to individual error, these data provide convincing evidence that the tape peeling methodology can yield accurate sequential isolations of rod photoreceptor layers for protein analysis.

FIGURE AND TABLE LEGENDS:

Figure 1: Schematic of the live cell peeling steps. (A) Diagram shows the main steps for dissecting and hemisecting the isolated eye. (B) Photoreceptor outer segments are removed incrementally by sequential peeling using filter paper. First, retinas are oriented so that the photoreceptor layer is in contact with the filter paper. Next, the filter paper is dried by blotting on a paper towel, and the retina is peeled away from the filter paper. This peeled isolate is collected in a tube kept on ice. This process is repeated seven to eight times to fully remove the rod outer segment (+ROS). This figure was created with BioRender.com.

Figure 2: Lyophilized retina peeling process. (A) Flow diagram of the sample preparation for the lyophilized retina. Retinas are oriented so that the retinal ganglion cell layer is in contact with the filter paper and the photoreceptors are facing up. (B) Post lyophilization, the freeze-dried retina is adhered to a piece of tape after adding slight pressure to the top of the tape. The tape is peeled away, removing the rod outer segment (ROS) and rod inner segment (RIS) layers. The RIS layer is removed by more tape peels until the ROS layer is visible (orange/pink layer). This figure was created with BioRender.com.

Figure 3: Expression of GNAT1 and ARR1 in isolated rod photoreceptors after sequential filter paper peeling. (A) Immunoblots of +ROS and -ROS (ROS-depleted) samples collected by the filter paper peeling method acquired from dark- and light-adapted retinæ. Blots were probed with antibodies for light-triggered proteins (transducin (GNAT1) and arrestin (ARR1)) and quality control markers (GTPase activating protein (Gβ5L/S) cytochrome C (Cyt C), and actin). Two halved retinæ were combined for these representative blots. (B) Quantified signals of GNAT1 and ARR1 from dark- and light-adapted retinæ. There is reciprocal light-triggered movement of GNAT1 and ARR from +ROS and -ROS isolates. Violin plots depict the normalized expression of +ROS and -ROS samples. This figure has been modified from Rose et al.³⁶.

Figure 4: Scanning electron microscope images of lyophilized retina. (A) Surface of lyophilized retina before tape peeling (photoreceptor side up). (B) The inner segment layer post tape peeling. (C) The cell body layer post tape peeling shows a uniform nuclear appearance. This figure has been modified from Rose et al.³⁶ and was created with [BioRender.com](https://www.biorender.com).

Figure 5: Validation of the tape peeling method to isolate ROS and RIS from lyophilized retina. (A) Western blots of +ROS, +RIS, and -OIS (ROS/RIS-depleted) samples collected by the tape peeling method. Immunoblots were probed with transducin (GNAT1), arrestin (ARR1), GTPase activating protein (Gβ5L/S), cytochrome C (Cyt C), and actin antibodies. Samples were obtained from dark- and light-adapted retinæ and halved retinal isolates (+ROS, +RIS, -OIS) were combined for more concentrated material. (B) Quantified signals of GNAT1 and ARR1 are plotted as violin plots for the different isolated retinal layers, which were obtained from dark- and light-adapted retinæ. (C) Normalized expression levels from +RIS and -OIS were combined and plotted to compare tape and filter paper peeling methods. Dark- and light-adapted samples displayed known movement of key phototransduction proteins. This figure has been modified from Rose et al.³⁶.

Figure 6: Tape peeling of lyophilized retina to investigate the subcellular localization of GRK1 and PKCα in photoreceptors. (A) A representative western blot of peeled samples from light-adapted C57BL/6J mice demonstrating the relative levels of rhodopsin kinase (GRK1), protein kinase C-alpha (PKCα), GTPase activating protein (Gβ5L/S), and actin. (B) Frozen retinal section prepared from light-exposed mice incubated with PKCα antibody (green, 1:100). RPE, retinal pigmented epithelium; OS, outer segment; IS, inner segment; CB, cell body; ST, synaptic terminal. Scale bar = 10 μm. (C) PKCα and GRK1 normalized expression levels for +ROS, +RIS, -OIS samples are plotted as violin plots. (D) Sub-optimal tape peeling could potentially yield slightly contaminated samples. The red square highlights the +RIS sample contaminated with some -OIS sample, producing both Gβ5L/S bands and a higher PKCα signal. Two halved retinæ were combined for all blots.

Table 1: List of antibodies used for western blot validation of separation techniques.

Table 2: Protein concentration in retinal isolation homogenates.

DISCUSSION:

Many retinal diseases affect rod photoreceptor cells, leading to rod death and, ultimately, complete vision loss³⁷. A significant portion of the genetic and mechanistic origins of human retinal degeneration have been successfully recapitulated in numerous mouse models over the years. In that context, the ability to easily and selectively separate individual rod subcellular compartments from the small mouse retina would greatly enhance our understanding of the localized biochemical and molecular underpinnings of retinal diseases. Furthermore, the layered nature of the neural retina, combined with the unique, highly polarized arrangement of rod photoreceptors, permits the isolation of rod compartments by selective peeling. This manuscript describes two protocols used to isolate individual subcellular compartments of rod photoreceptor cells for immunoblotting. Not only are both methods considerably faster and less technically challenging when compared to the existing method of tangential sectioning⁹, but they also require a substantially smaller sample size than the common biochemical isolation of the ROS using density gradients¹⁹. Such ROS gradient purification techniques require 8–10 murine retinæ to reliably recover ample ROS, whereas the protocols presented here are suitable for single retinæ.

Despite the overall simplicity of the proposed techniques, one of the main challenges common to both protocols concerns the flattening of the curved retina onto the filter paper required for proper isolation of the different subcellular compartments. The isolated retina tends to curl up and take on a clam-like shape. If the retina has folded edges when placed on the filter paper (photoreceptor side either up or down), this may decrease the yield of the desired isolated rod layers. More importantly, if the retina is not properly flattened, then layer misalignment and contamination from other subcellular compartments and retinal cells is a likely outcome (**Figure 6D**). To limit the curvature of the halved retinal rectangle and to rectify the imperfect alignment of the rod and retinal layers, the retinal rectangle can be cut in half to produce two retinal squares. By cutting the neural retina into smaller pieces, the natural curvature of the retina is reduced, and the tissue is more likely to lay flat on the filter paper.

Recognizing when the different rod compartments have been physically separated can be tricky for someone inexperienced with these techniques. We advise that before commencing a biologically significant experiment, the user should run through the process with sample retinæ for an hour or two. Practice should result in substantial improvement in the operator's skills and proficiency in the methods. When using filter paper to peel away the ROS from a live retina, no obvious visual cues indicate when the ROS layer has been isolated. While the retina becomes thinner and more fragile, the user will have to self-monitor and validate the number of peels to isolate the ROS accurately. Furthermore, using filter paper with different fiber thicknesses and coarseness will alter the ROS peeling time. Filter paper with thicker fibers (such as VWR Grade 413) will isolate retinal layers faster (6–8 peels), but may not be as selective and can lead to contamination from other layers. Filter paper with thinner fibers (such as Whatman Grade 1) will isolate retinal layers slower (12–15 peels) and will give a clean isolation of the photoreceptor layers. We recommend using both thicker and thinner filter paper to minimize the peeling time and ensure collection purity.

At the same time, visual approximation and tape sample handling are both key to the success of isolating the subcellular compartments from the lyophilized retina. If too much pressure is added to the tape, the entire lyophilized retina will adhere to the tape. Once this occurs, separating the ROS becomes lengthier and more difficult, but not impossible: place a second piece of tape on the free surface (on the ganglion cell side) of the retina and slowly pull away the layers with tape until only the orange/pinkish layer is visible on the initial piece of tape. Isolating the RIS at this point, however, is impossible. If too little pressure is added to the tape, a large portion of the ROS will not adhere to the tape. To ensure proper ROS-tape adhesion, we advise gently pressing with tweezers on the regions that are not sticking to the tape. Typically, the slightest pressure results in the removal of the ROS and RIS layers, however, the amount of pressure must be determined based on experience. The presence of isolated RIS can be ascertained by checking whether a thin, white layer (akin to a light dusting of snow) is visible on the initial ROS tape peel, while the presence of isolated ROS can be easily determined by checking the color of the rod photoreceptor layer (orange for dark-adapted, pinkish for light-adapted) on the tape.

One final challenge arises when homogenizing the filter paper peels (+ROS) from the live retina. Filter paper easily absorbs liquid, and a considerable amount of the homogenizing buffer will be soaked up during this step of the protocol. Spinning the liquid down in a mini centrifuge after placing the peeling paper on the side of each tube helps prevent the loss of sample. Unfortunately, spinning down multiple pieces of filter paper can be a time-consuming process, and loss of sample is inevitable. To address this issue, remove some of the filter paper pieces and focus on homogenizing fewer pieces at a time. Additionally, to avoid the loss of sample during this step, consider minimizing the total amount of filter paper used to isolate the ROS.

While both our methods do not require a large sample size, or the precise alignment of a blade to section the retina, there are a few limitations to our photoreceptor peeling techniques that are worth noting. First, the lyophilized murine retina may not be amenable for peeling subsequent photoreceptor layers beyond the ROS and RIS. Second, our peeling methods are more suited for processing individual retinæ and are not amenable to large batch processing in one sitting. Third, the success of the experiment is dependent on the sensitivity limit of the antibody used in the western blot. Despite these limitations, our representative results demonstrate that our two isolation peeling techniques can efficiently isolate specific rod photoreceptor compartments. Additionally, these two methods use inexpensive and commonplace lab materials (filter paper and adhesive tape), making them highly accessible. In our study, we did not directly assess whether other retinal cells could be isolated for immunoblotting; however, we believe that these methods may be easily modified to benefit the needs of a broad cross-section of the retinal research community.

ACKNOWLEDGMENTS:

This work was supported by NIH Grant EY12155, EY027193, and EY027387 to JC. We are thankful to Dr. Spyridon Michalakis (Caltech, Pasadena, USA) and Natalie Chen (USC, Los Angeles, USA) for proofreading the manuscript. We would also like to thank Dr. Seth Ruffins (USC, Los Angeles, USA) and Dr. Janos Peti-Peterdi (USC, Los Angeles, USA) for providing the necessary equipment to collect the author provided footage. Material from: Kasey Rose et al, Separation of

photoreceptor cell compartments in mouse retina for protein analysis, *Molecular Neurodegeneration*, published [2017], [Springer Nature].

DISCLOSURES:

The authors declare that they have no competing interests.

REFERENCES:

1. Arshavsky, V. Y., Lamb, T. D., Pugh, E. N. G proteins and phototransduction. *Annual Review of Physiology*. **64**, 153–187 (2002).
2. Molday, R. S., Moritz, O. L. Photoreceptors at a glance. *Journal of Cell Science*. **128** (22), 4039–4045 (2015).
3. Koch, K. W., Dell'Orco, D. Protein and signaling networks in vertebrate photoreceptor cells. *Frontiers in Molecular Neuroscience*. **8**, 67 (2015).
4. Semple-Rowland, S. L., Dawson, W. W. Cyclic light intensity threshold for retinal damage in albino rats raised under 6 lx. *Experimental Eye Research*. **44** (5), 643–661 (1987).
5. Brann, M. R., Cohen, L. V. Diurnal expression of transducin mRNA and translocation of transducin in rods of rat retina. *Science*. **235** (4788), 585–587 (1987).
6. Philp, N. J., Chang, W., Long, K. Light-stimulated protein movement in rod photoreceptor cells of the rat retina. *FEBS Letters*. **225** (1–2), 127–132 (1987).
7. Broekhuysse, R. M., Tolhuizen, E. F., Janssen, A. P., Winkens, H. J. Light induced shift and binding of S-antigen in retinal rods. *Current Eye Research*. **4** (5), 613–618 (1985).
8. Roof, D. J., Heth, C. A. Expression of transducin in retinal rod photoreceptor outer segments. *Science*. **241** (4867), 845–847 (1988).
9. Sokolov, M. et al. Massive light-driven translocation of transducin between the two major compartments of rod cells: a novel mechanism of light adaptation. *Neuron*. **34** (1), 95–106 (2002).
10. Lobanova, E. S. et al. Transducin translocation in rods is triggered by saturation of the GTPase-activating complex. *The Journal of Neuroscience*. **27** (5), 1151–1160 (2007).
11. Strissel, K. J., Sokolov, M., Trieu, L. H., Arshavsky, V. Y. Arrestin translocation is induced at a critical threshold of visual signaling and is superstoichiometric to bleached rhodopsin. *The Journal of Neuroscience*. **26** (4), 1146–1153 (2006).
12. Nair, K. S. et al. Light-dependent redistribution of arrestin in vertebrate rods is an energy-independent process governed by protein-protein interactions. *Neuron*. **46** (4), 555–567 (2005).
13. Strissel, K. J. et al. Recoverin undergoes light-dependent intracellular translocation in rod photoreceptors. *The Journal of Biological Chemistry*. **280** (32), 29250–29255 (2005).
14. Calvert, P. D., Strissel, K. J., Schiesser, W. E., Pugh, E. N., Arshavsky, V. Y. Light-driven translocation of signaling proteins in vertebrate photoreceptors. *Trends in Cell Biology*. **16** (11), 560–568 (2006).
15. Majumder, A. et al. Transducin translocation contributes to rod survival and enhances synaptic transmission from rods to rod bipolar cells. *Proceedings of the National Academy of Sciences of the United States of America*. **110** (30), 12468–12473 (2013).
16. Fain, G. L. Why photoreceptors die (and why they don't). *BioEssays*. **28** (4), 344–354 (2006).
17. Chen, J., Simon, M. I., Matthes, M. T., Yasumura, D., LaVail, M. M. Increased susceptibility to light damage in an arrestin knockout mouse model of Oguchi disease (stationary night

- blindness). *Investigative Ophthalmology & Visual Science*. **40** (12), 2978–2982 (1999).
18. Song, X. et al. Arrestin-1 expression level in rods: balancing functional performance and photoreceptor health. *Neuroscience*. **174** 37–49 (2011).
19. McConnell, D. G. The isolation of retinal outer segment fragments. *The Journal of Cell Biology*. **27** (3), 459–473 (1965).
20. Tsang, S. H. et al. Role for the target enzyme in deactivation of photoreceptor G protein in vivo. *Science*. **282** (5386), 117–121 (1998).
21. Walston, S. T., Chow, R. H., Weiland, J. D. Patch clamp recordings of retinal bipolar cells in response to extracellular electrical stimulation in wholemount mouse retina. *Annual International Conference of the IEEE Engineering in Medicine and Biology Society*. **2015**, 3363–3366 (2015).
22. Guido, M. E. et al. A simple method to obtain retinal cell preparations highly enriched in specific cell types. Suitability for lipid metabolism studies. *Brain Research. Brain Research Protocols*. **4** (2), 147–155 (1999).
23. Hayashi, F. et al. Phosphorylation by cyclin-dependent protein kinase 5 of the regulatory subunit of retinal cGMP phosphodiesterase. II. Its role in the turnoff of phosphodiesterase in vivo. *The Journal of Biological Chemistry*. **275** (42), 32958–32965 (2000).
24. Wolbring, G., Cook, N. J. Rapid purification and characterization of protein kinase C from bovine retinal rod outer segments. *European Journal of Biochemistry*. **201** (3), 601–606 (1991).
25. Williams, D. S. et al. Characterization of protein kinase C in photoreceptor outer segments. *Journal of Neurochemistry*. **69** (4), 1693–1702 (1997).
26. Watson, A. J., Aragay, A. M., Slepak, V. Z., Simon, M. I. A novel form of the G protein beta subunit Gbeta5 is specifically expressed in the vertebrate retina. *The Journal of Biological Chemistry*. **271** (45), 28154–28160 (1996).
27. Makino, E. R., Handy, J. W., Li, T., Arshavsky, V. Y. The GTPase activating factor for transducin in rod photoreceptors is the complex between RGS9 and type 5 G protein beta subunit. *Proceedings of the National Academy of Sciences of the United States of America*. **96** (5), 1947–1952 (1999).
28. Chen, J., Shi, G., Concepcion, F. A., Xie, G., Oprian, D. Stable rhodopsin/arrestin complex leads to retinal degeneration in a transgenic mouse model of autosomal dominant retinitis pigmentosa. *The Journal of Neuroscience*. **26** (46), 11929–11937 (2006).
29. Chen, C. K. et al. Abnormal photoresponses and light-induced apoptosis in rods lacking rhodopsin kinase. *Proceedings of the National Academy of Sciences of the United States of America*. **96** (7), 3718–3722 (1999).
30. Zhang, H. et al. Mistrafficking of prenylated proteins causes retinitis pigmentosa 2. *FASEB Journal*. **29** (3), 932–942 (2015).
31. Weiss, E. R. et al. Species-specific differences in expression of G-protein-coupled receptor kinase (GRK) 7 and GRK1 in mammalian cone photoreceptor cells: implications for cone cell phototransduction. *The Journal of Neuroscience*. **21** (23), 9175–9184 (2001).
32. Zhao, X., Huang, J., Khani, S. C., Palczewski, K. Molecular forms of human rhodopsin kinase (GRK1). *The Journal of Biological Chemistry*. **273** (9), 5124–5131 (1998).
33. Newton, A. C., Williams, D. S. Involvement of protein kinase C in the phosphorylation of rhodopsin. *The Journal of Biological Chemistry*. **266** (27), 17725–17728 (1991).
34. Pinzon-Guzman, C., Zhang, S. S., Barnstable, C. J. Specific protein kinase C isoforms are

787 required for rod photoreceptor differentiation. *The Journal of Neuroscience*. **31** (50), 18606–
788 18617 (2011).

789 35. Sokal, I. et al. Identification of protein kinase C isozymes responsible for the
790 phosphorylation of photoreceptor-specific RGS9-1 at Ser475. *The Journal of Biological Chemistry*.
791 **278** (10), 8316–8325 (2003).

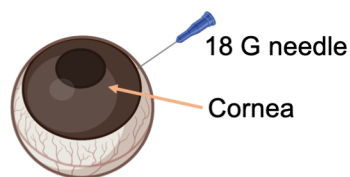
792 36. Rose, K., Walston, S. T., Chen, J. Separation of photoreceptor cell compartments in mouse
793 retina for protein analysis. *Molecular Neurodegeneration*. **12** (1), 28 (2017).

794 37. Wright, A. F., Chakarova, C. F., Abd El-Aziz, M. M., Bhattacharya, S. S. Photoreceptor
795 degeneration: genetic and mechanistic dissection of a complex trait. *Nature Reviews. Genetics*.
796 **11** (4), 273–284 (2010).

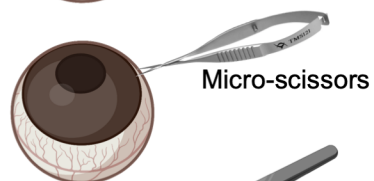
797

A

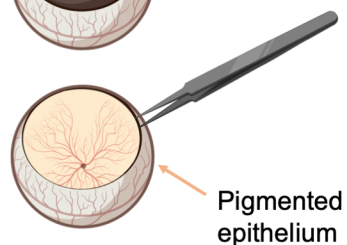
Puncture cornea-limbus junction



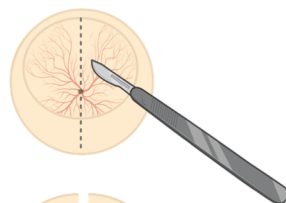
Remove cornea



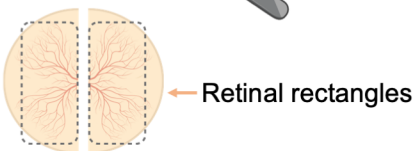
Peel pigmented epithelium



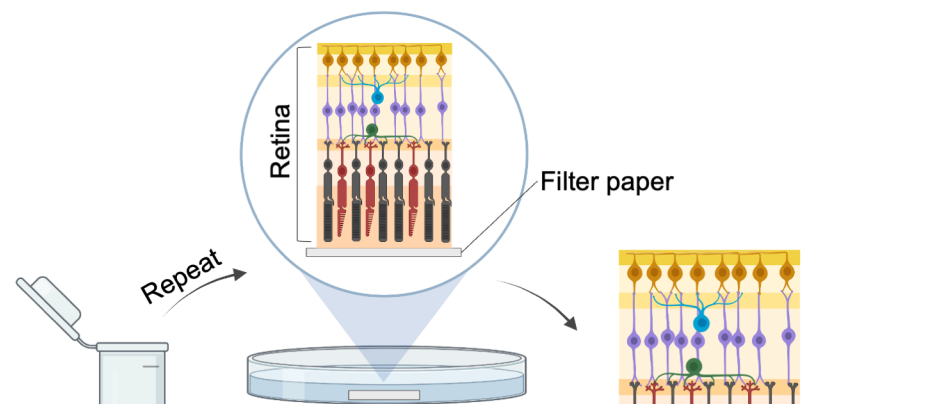
Bisect retina



Trim edges

**B**

1. Create retina-filter paper adhesion

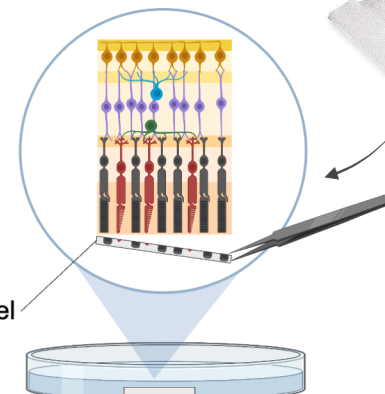


4. Store peel in tube

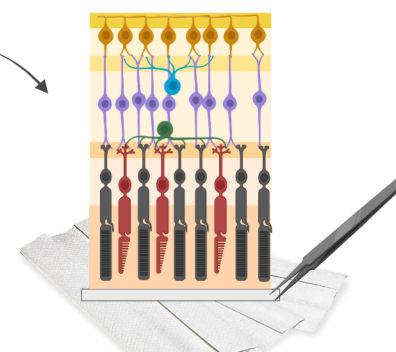


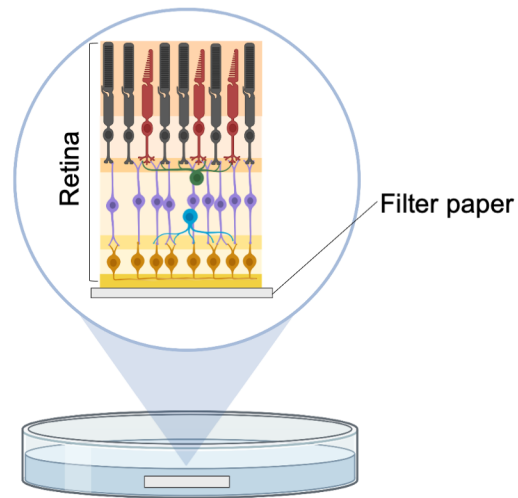
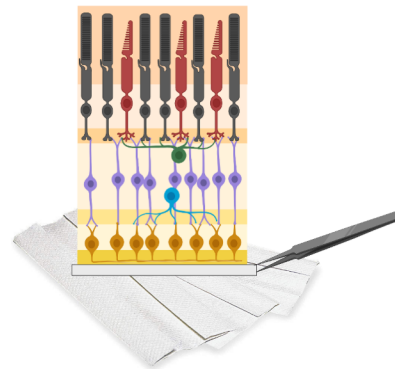
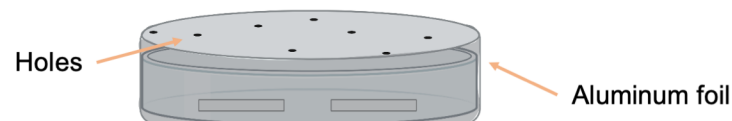
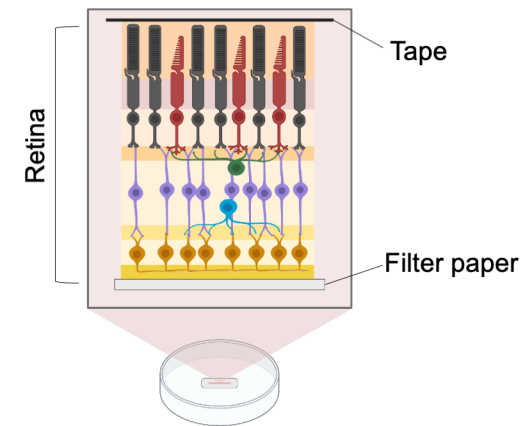
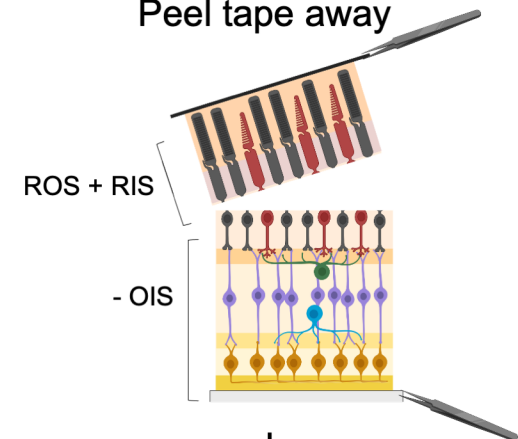
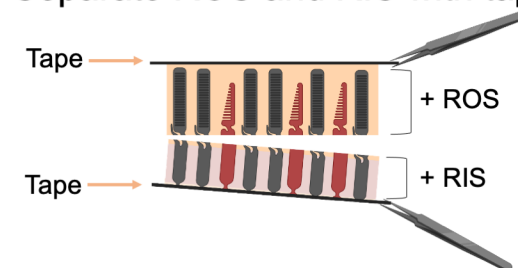
+ROS peel

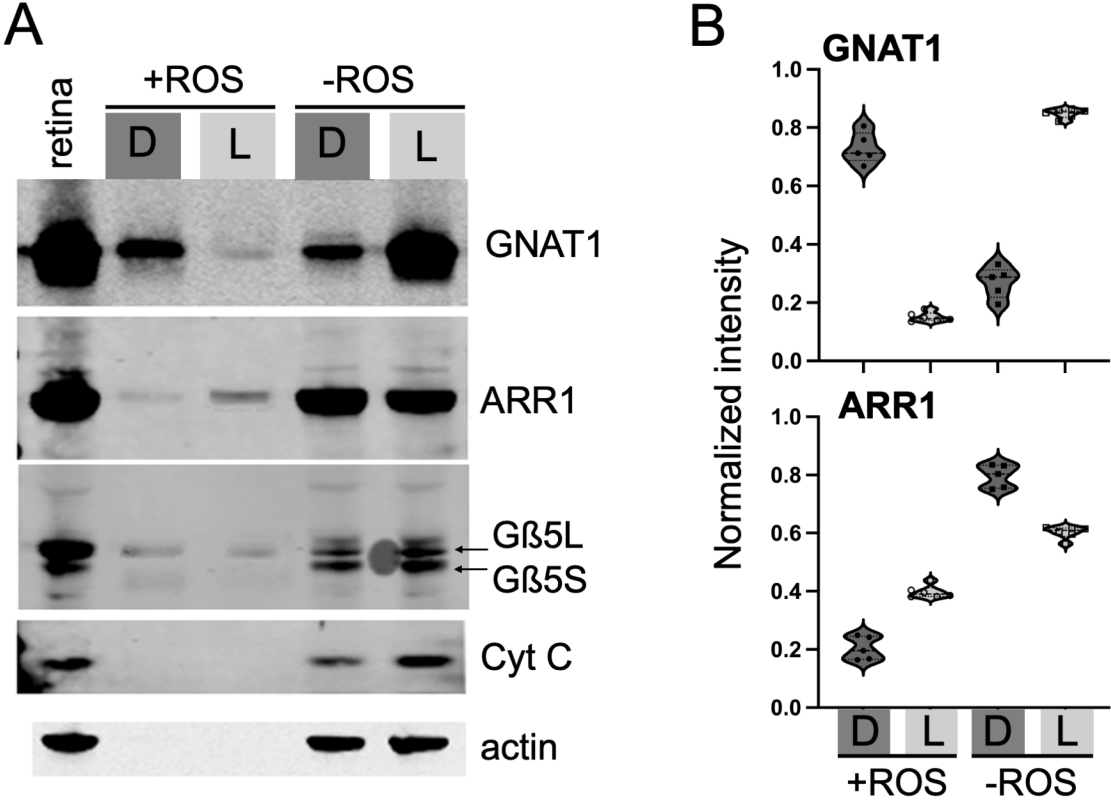
3. Peel retina away from filter paper

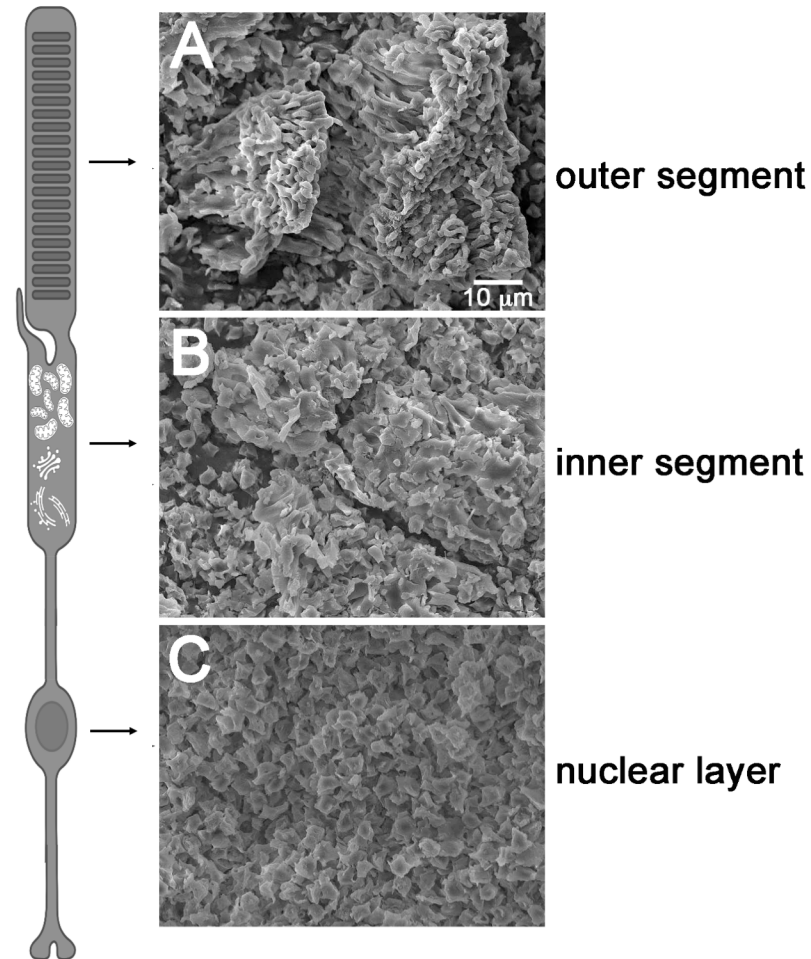


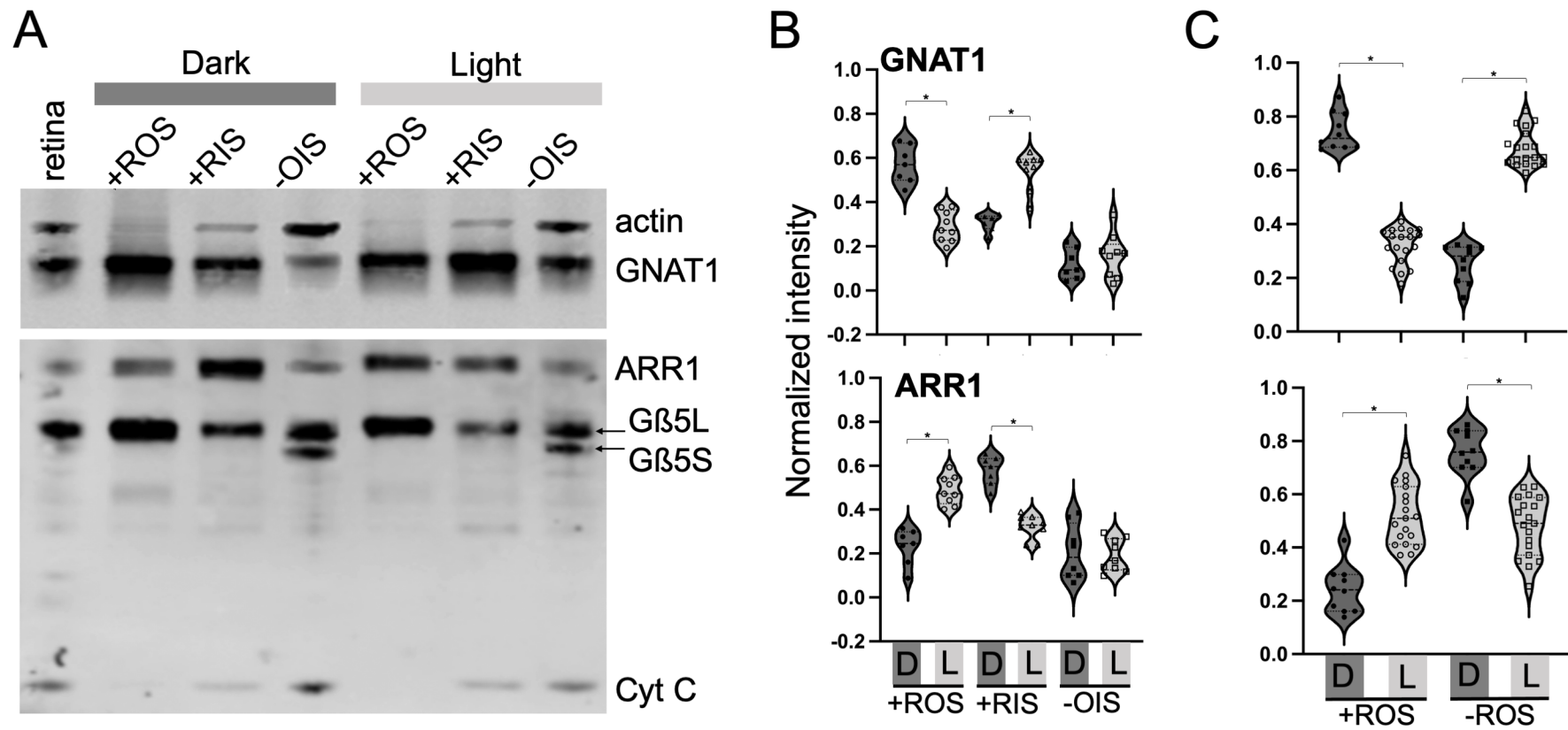
2. Blot on paper towel

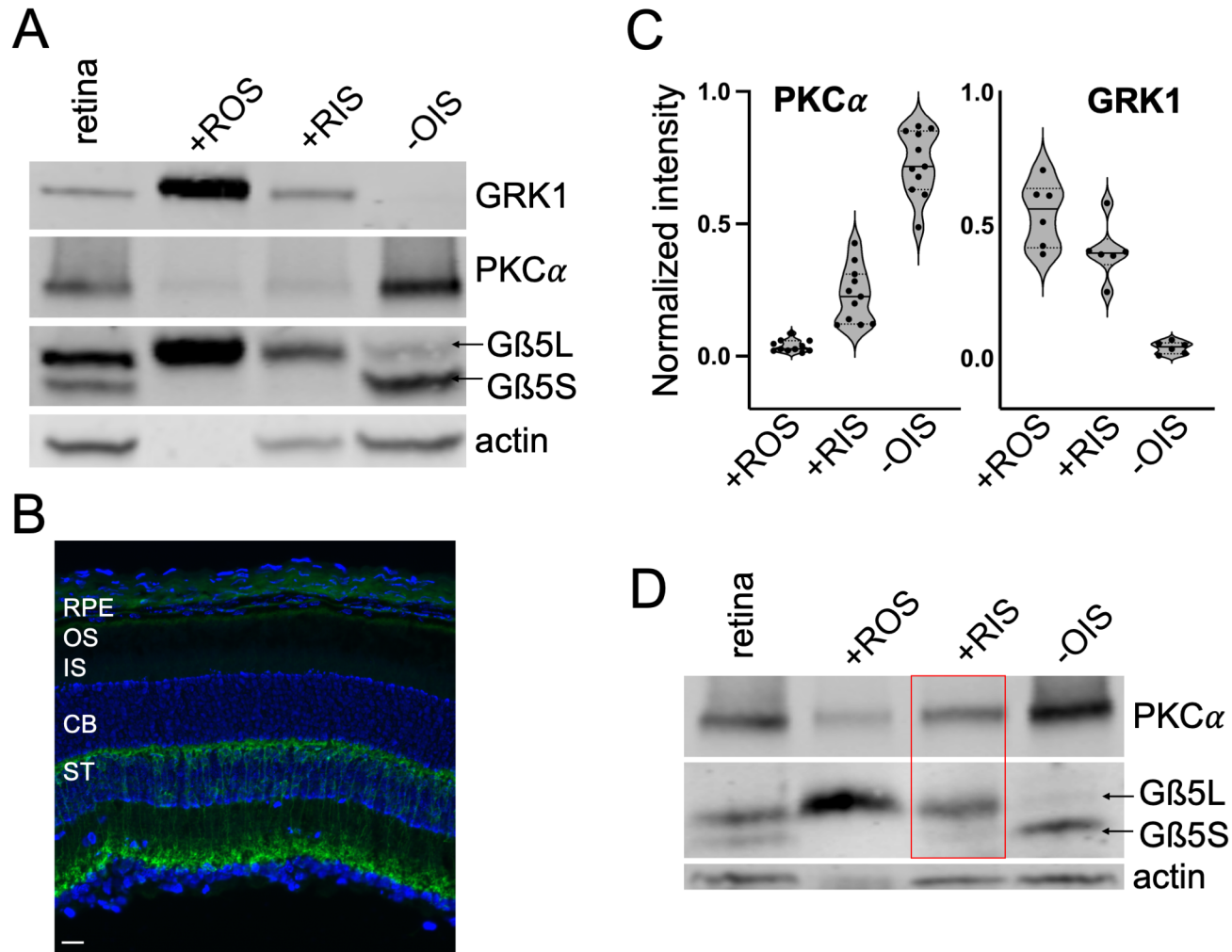


A**Create retina-filter paper adhesion****Blot on paper towel****Cover samples, freeze in liquid nitrogen, and lyophilize****B****Place tape on lyophilized retina****Peel tape away****Separate ROS and RIS with tape**





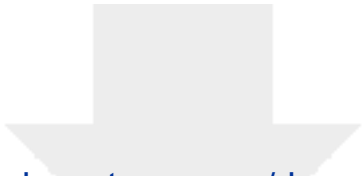




Target	Antibody	Dilution	Manufacturer
Arrestin	Rabbit anti-ARR1	1:1000	Chen, <i>et. al.</i> , 2006.
Transducin	Mouse anti-GNAT (TF-15)	1:1000	CytoSignal.
β Actin	Rabbit anti- β Actin	1:5000	GeneTex Inc.
Cytochrome C	Rabbit anti-cytochrome C	1:500	Santa Cruz, sc-7159.
GAP (G β 5L/S)	Rabbit anti-G β 5L/S (CT2-15)	1:2000	Watson, <i>et. al.</i> , 1996.
Protein kinase C alpha (PKC)	Rabbit anti-PKC (#2050)	1:1000	Cell Signaling Technology.
Rhodopsin Kinase (GRK1)	Mouse anti-GRK1 (G-8)	1:200	Santa Cruz, sc-8004.

Filter paper retinal isolation				
	+ROS [*]		-ROS [*]	Whole Retina
Average protein concentration (µg/mL)	700		1,500	1,500
RIPA buffer volume (µL)	90		150	200
Tape peeling retinal isolation				
	+ROS [*]	+RIS [*]	-ROS [*]	Whole Retina
Average protein concentration (µg/mL)	520	440	1,200	1,600
RIPA buffer volume (µL)	100	100	125	150

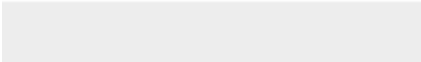
^{*}Combined two halved retinal isolations.



[Click here to access/download](#)

Table of Materials

Copy of JoVE_Materials (1).xlsx



We thank the reviewers for their constructive comments and feedback. In response, we have edited the manuscript to address their concerns and have added new data and experiments.

Reviewer 1

Reviewer 1 – minor concerns

1. **Abstract: change**
 studythmovement > study the movement
 However,the > However, the
 Recently,motivated > Recently, motivated
 Ofproteintransportbetween > of protein transport between
 compartments,wedeveloped > compartments, we developed
 forWestern blots. > for western blots.
 Thank you. Done.
2. **Manuscript: change**
 Line 78 Western Blot > western blot
 Line 78 C57BL/6 C57BL/6N or C57BL/6J
 Lines 106-107: 4 °C > 4°C
 Lines 115 15 mins > 15 min
 Line 124 Institutional Animal Care and Use Committee (IACUC)
 Line 360 50mM > 50 mM
 Line 361 150mM > 150 mM
 Line 361 1mM > 1 mM
 Line 364 -20 °C > -20°C
 Line 367 0.1M > 0.1 M
 Line 373-404 -80 °C > -80°C
 Line 423 bichinchoninic acid assay (BCA)
 Line 427 Western bot > western blot
 Line 598 Western bot > western blot
 Thank you. Done.
3. **Lines 142-160-250 You must specify the orientation**
 We have added wording to specify the orientation of the retina.
4. **Line 412 IOS must be defined**
 We have defined OIS for clarity.
5. **Figure 3 The two graphs of figure 3B must be aligned vertically**
 We have vertically aligned Fig. 3B graphs.

Reviewer 2

Reviewer 2 – major concerns

1. **Although it is stated in JOVE's publication criteria that "novelty is NOT a requirement for publication", there are concerns that in the present case the concept of novelty has been overtaken with a more serious form of re-presenting previously published results and figures by the same authors. That would be the case unless this current submission**

is intended to be a Review, which it is clearly not. The current submission states that this work extends from citation 22 (Walston, S. T., Chow, R. H. & Weiland, J. D.). In fact, the current submission recapitulates citation #28 [Rose, K., Walston, S. T. & Chen, J. Separation of photoreceptor cell compartments in mouse retina for protein analysis. *Mol Neurodegener.* 12 (1), 28, doi:10.1186/s13024-017-0171-2, (2017)], which has two of the same authors (Rose and Chen) and which includes a "JOVE-like" video (but with music instead of narration) showing the steps for using sequential scotch tape peeling of a mouse retina into what appears to be the same layers discussed in the present submission, and overlaps significantly with the current submission. If the authors will clarify, point by point, what facts differentiate and discriminate citation 28 from the current submission in a manner that supports re-presentation of a method paper in the form of this publication, it will be greatly appreciated.

Thank you for your feedback, and you are correct that these two separation protocols have been published previously. When JoVE reached out to us about their current endeavor to create a PubMed-indexed collection of video articles on the 'Current Methods in Eye Research,' we liked the idea of making our simple isolation protocols available on the JoVE platform. JoVE is the leading producer of scientific video protocols and working with them will help us reach a wider audience and add value to the retinal isolation space. This current iteration does not violate [Springer Nature's Copyright and Licensing agreement](#). With that being said, while we decided to keep the previously published data showing how these techniques can reliably, quickly, and easily separate rod subcellular compartments, we have also added additional experiments in response to your concerns.

We have added an entirely new figure to the manuscript (Fig. 6) to show another application of the tape-peeling technique. Because different experimental methods (ICC and western blot) yield conflicting results about the localization of rhodopsin kinase (GRK1) and protein kinase C-alpha (PKC α) within the retina, we decided to use our technique to investigate the localization of rhodopsin kinase (GRK1) and protein kinase C-alpha (PKC α) within the ROS, RIS, and ROS/RIS-deficient samples. We also used G β 5S/G β 5L and actin as important loading controls (which we had used in our other western blots). Our method allowed us to selectively isolate the GRK1 signal in the ROS of light-exposed mice (Fig. 6A). The absence of GRK1 signal in the -OIS sample confirms the ROS has been isolated from the rest of the retina, and that previous data showing immunostaining of the rest of the rod is an artifact or is due to non-specific staining. This example helps show how our tape peeling technique produces enriched subcellular fractions for western blot analysis. Next, we decided to show how our technique can investigate lesser-known photoreceptor proteins, such as PKC α . Several studies have presented functional and biochemical data supporting the presence of PKC α in rods, but typically the expression in ICC is lacking (it only labels bipolar cells). We decided to investigate if we could use our technique to recapitulate known data surrounding PKC α in rods. We found that there is slight expression of PKC α in the ROS and RIS samples (Fig. 6A), and its expression in rods was not visible in ICC (Fig. 6B). We next normalized and plotted the data for the GRK1 (n=8) and PKC α (n=11) signals from these blots. Our data consistently shows how reliable our isolation method is in isolating specific compartments

for specific proteins (Fig. 6C). Lastly, we added a representative blot showing a sub-optimal tape peeling session to demonstrate how contamination from different sub-layers (specifically the -OIS isolation contaminating the +RIS sample) can affect results and how the data is interpreted (Fig. 6D).

2. **Fig 3AB is the identical data with slightly modified graphs from Rose et al, 2017 Fig 2BC. The current figure legend does state "reproduced with permission from Springer Nature²⁸". Fig 4 is the identical data with slightly modified graphs from the 2017 paper's Fig 3. The current figure legend also states "reprinted with permission from Springer Nature²⁸". Fig 5ABC is the identical data with slightly modified graphs from the 2017 paper's Fig 4ABC. The current figure legend does not state "reprinted with permission from Springer Nature".**

Thank you for pointing this out. We have reached out to Springer Nature Group for further clarification about how to correctly cite previously published figures or tables. According to Springer Nature Group, "reproduction of figures or tables from any open access article is permitted free of charge and without formal written permission from the publisher or the copyright holder, provided that the figure/table is original and following are included in the acknowledgement section 1) the Copyright license the material is published, 2) the publisher's name is duly identified as the original publisher, and 3) the proper attribution of authorship and the correct citation details are given." Considering this information, we have updated our Acknowledgement section to fulfill this requirement. Moreover, we have added 'This figure has been modified from Rose et al.²⁸' in the figure legend for Figures 3-5.

Reviewer 2 – minor concerns

1. **Poor writing throughout.**

Experienced writers, who are native English speakers, have edited and proofread this manuscript. We are happy to correct specific instances of poor writing, but it is not possible to address this further unless we are given more specific examples. In light of this comment, we have thoroughly examined and edited this iteration of the manuscript.

2. **Unedited writing left 'phototransduction' defined on line 34 as 'a prototypical G-protein signaling cascade', hardly the case given the role of cGMP activating a channel.**

We have considered this suggestion and changed the sentence to the following: "To function as faithful photon counters, rods utilize a G-protein-based signaling pathway, termed phototransduction, to generate rapid, amplified, and reproducible responses to single photon capture."

3. **'ST' is defined as synapse in line 36 as 'synapse' (whereas surely it should be 'synaptic terminal'), and is redefined on line 39 as 'synaptic transmission'.**

Thank you. We have re-written for clarity. 'Synapse' is now 'synaptic terminal' and we have removed 'ST' after 'synaptic transmission'.

4. **Line 150: Fix "carbongenated".**

Both 'carbongenated' and 'carbongenated' are two forms of spelling that are typically used for 95% O₂/5% CO₂. We have decided to change 'carbongenated' to 'carbongenated' within the manuscript.

Reviewer 3

Reviewer 3 – minor concerns

1. **The abbreviation of the rod outer segment (ROS) and rod inner segment (RIS) should be included at the beginning of the manuscript.**

We have added and defined ROS and RIS in the Introduction section of the manuscript.

2. **In point 2. Dissection of the Retina, between 3.2 and 3.3, there is missing the retinal extraction step from the cornea-choroid-RPE.**

We have updated our 'Dissection of the Retina' subsection (1.2) to include the removal of the retinal pigmented epithelium (RPE)-sclera-choroid complex.

3. **In section 2. Lyophilized Retina Peeling Method, 3.3.4 "Place all filter paper pieces into the 35 x 10 mm petri dish", I wonder whether the plastic petri dish is prepared to withstand the liquid nitrogen.**

We are aware that plastic petri dishes may become brittle and can easily break when introduced into liquid N₂. However, our samples are placed in liquid N₂ for ~ 10 mins (just right before the lyophilization step), and we have not experienced any cracking or breakage of our dishes during this short storage time in liquid N₂. We have not stored or submerged our samples in liquid N₂ for prolonged periods of time and do not know how these petri dishes would hold up.

4. **3.3.5. "Use metal tongs, gradually lower the aluminum foil-covered petri dish into the liquid nitrogen", I wonder whether the foil is hooked enough not to get up when it goes under de liquid N₂.**

Thank you for this observation. We have noted that this description was unclear and clarified the process of fully covering the petri dish with aluminum foil in the subsection 2.3.12.

5. **In the results, only ROS-specific markers are used to prove the protocol's efficiency. However, I missed more controls such as photoreceptor nuclear and synaptic markers to prove that neither ONL nor OPL is present, or other non-photoreceptor markers, such as bipolar PKC α to prove that the bipolar layer is not peeled out together with RIS. This would be useful for a newly non-experienced researchers who will implement this technique.**

Thank you for the suggestion. We have followed your recommendation and added PKC α western blot data to investigate if fractions were contaminated by the OPL. We were surprised to find that there was a low expression of PKC α in ROS and RIS fractions. After further investigation into previous work investigating PKC α expression in rods, we found that there are functional and biochemical data supporting the presence of PKC α in rods (we referenced these articles in the manuscript). PKC α expression in rods is consistently unable to be detected by immunocytochemistry (ICC), potentially due to epitope masking. Because of this, we believe our separation technique for western blot can be advantageous compared to ICC for investigating known and unknown proteins within rod photoreceptor compartments.

The article (<https://doi.org/10.1186/s13024-017-0171-2>) was published under a CC BY license so authors are not required to obtain permission to reuse this article, as shown [here](#) or seen in picture below.



The screenshot shows the Springer Nature RightsLink interface. At the top, the 'CCC | RightsLink' logo is on the left, and 'Help' and 'Email Support' links are on the right. The main content area displays the article title 'Separation of photoreceptor cell compartments in mouse retina for protein analysis' by Kasey Rose et al. It lists the publication as 'Molecular Neurodegeneration', the publisher as 'Springer Nature', and the date as 'Apr 11, 2017'. Below this, the 'Creative Commons' section states that the article is distributed under a CC BY license, allowing unrestricted use, distribution, and reproduction in any medium, provided the original work is properly cited. It also notes that users are not required to obtain permission to reuse the article and that CC0 applies for supplementary material. At the bottom, there is a footer with copyright information: '© 2021 Copyright - All Rights Reserved | Copyright Clearance Center, Inc. | Privacy statement | Terms and Conditions' and a comment box: 'Comments? We would like to hear from you. E-mail us at customer@copyright.com'.

To learn more about copyright and licensing for BMC (a part of Springer Nature), please visit [this page](#).